Extensional basin geometry and elastic lithosphere

Article *in* Philosophical Transactions of The Royal Society A Mathematical Physical and Engineering Sciences · April 1999

DOI: 10.1098/rsta.1999.0351

CITATIONS
110

READS
757

4 authors, including:

Cindy Ebinger
Tulane University
267 PUBLICATIONS **13,238** CITATIONS

SEE PROFILE

THE ROYAL SOCIETY

Extensional basin geometry and the elastic lithosphere

By C. J. Ebinger[1]†, J. A. Jackson[2], A. N. Foster[2]‡ and N. J. Hayward[1]¶

[1]*School of Earth Sciences, University of Leeds, Leeds LS2 9JT, UK*
[2]*Department of Earth Sciences, Bullard Laboratories, University of Cambridge, Cambridge CB3 0EZ, UK*

Although the morphology and dimensions of continental rift basins vary considerably worldwide, one aspect is similar; tectonically active rifts are bordered on one or both sides by relatively long (tens of kilometres) normal fault systems (termed border faults) that largely control basin morphology. We compile data constraining the geometry of border faults within the tectonically active East African Rift system, and evaluate these results with respect to variations in thickness of the elastic lithosphere. Border-fault lengths greater than 75 km occur in regions with deep crustal seismicity and relatively high estimates of effective elastic thickness (T_e) derived from forward and inverse models of gravity and topography data ($T_e > 25$ km). Most East African border faults cross-cut pre-existing structures and basement foliations, although segments of the longest faults (greater than 80 km) reactivate Precambrian shear zones or structural fabrics. From observations in East Africa, comparisons with data from the Aegean and Baikal Rifts, and considerations of the rheology of continental lithosphere, we propose that the elastic lithosphere determines the length, width and style of faults within East Africa, and perhaps other continental rifts.

Keywords: border fault; continental rift; seismicity; rheology; East Africa; elastic thickness

1. Introduction

Continental lithosphere undergoing extension develops basins bounded on one or both sides by normal faults, but the dimensions and internal structure of these basins vary along the length of rift systems, as well as between rift systems worldwide (see, for example, Rosendahl 1987; Jackson & White 1989; Ruppel 1995). In cross-section, a majority of tectonically active continental rift basins shows a half graben morphology, with most of the strain accommodated along the border, or master, fault bounding the deep side of the basin (e.g. figure 1*a*). In plan view, displacement decreases toward the tips of border faults where they interact with faults bounding adjacent basins and/or transfer faults accommodating differential horizontal and vertical displacements between rift basins (see, for example, Trudgill & Cartwright

† Present address: Department of Geology, Royal Holloway College, University of London, Egham TW20 0EX, UK.

‡ Present address: Esso Exploration and Production UK, Mailpoint 25, Esso House, Ermyn Way, Leatherhead KT22 8UY, UK.

¶ Present address: Expro IS, Shell UK Exploration, 1 Altens Farm Rd, Aberdeen AB1 3FY, UK.

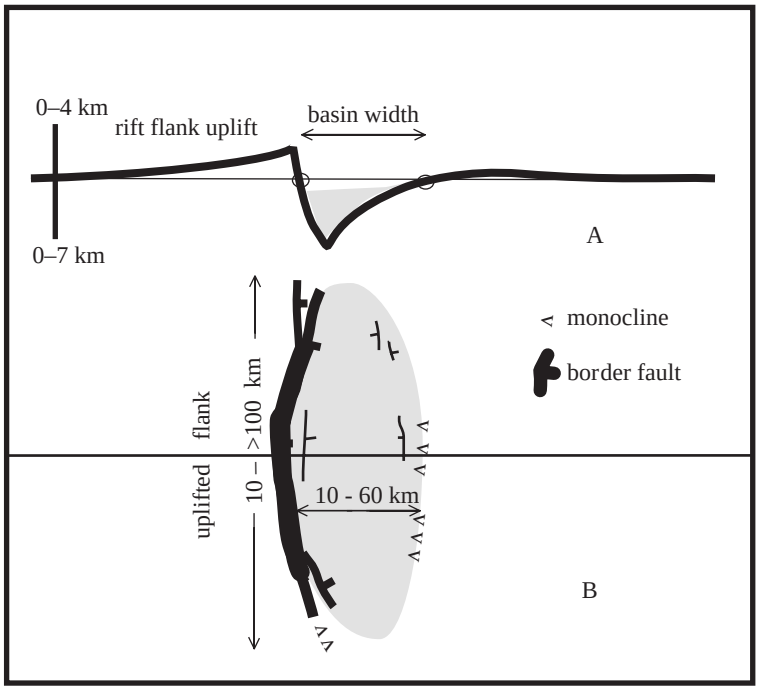

Figure 1. Generalized form of tectonically active continental rift basins showing border faults in cross-section (*a*) and plan form (*b*). (*a*) Most single-phase rift basins are half graben, with most of the deformation accommodated by slip along the border fault. Flexural isostatic compensation leads to uplift of the rift flanks, with the breadth and height dependent upon the strength of the elastic plate, and, to a lesser extent, β and the density of infilling material (see, for example, Weissel & Karner 1989). The lower relief margin is commonly faulted, or is a monocline dipping toward the basin. We measure the breadth of basins using the mean level of topographic relief *ca.* 200 km away from the basin, as indicated by the open circles. (*b*) Border faults show maximum displacement near the centre of the segment, with decreasing throws toward their tips usually taken up by several smaller faults, or by monoclines. The approximate line of (*a*) is shown by the light line. The elliptical area of depression is shown by shading.

(1994); and figure 1*b*). The geometry of border faults at mid- to lower crustal levels, however, is poorly constrained.

Within the fault population of any one basin, the border faults are usually the longest faults and have the greatest displacement. Shorter smaller offset faults often are seen in the hanging wall of the border fault (see, for example, Hayward & Ebinger 1996). Seismicity data show that deformation is concentrated along the border-fault system, since the largest earthquakes occur along the longest faults (see, for example, Roberts & Jackson 1991). Thus, border faults are the principal tectonic component of rift basins, and they provide insights into the deformational behaviour of the continental lithosphere. As demonstrated in this comparison of representative border faults in the East African, Aegean and Baikal Rifts, the lengths of border faults differ by a factor of four between rift systems, a difference we attribute to variations in thickness of the elastic lithosphere.

Jackson & White (1989) suggest a positive correlation between

(1) the thickness of the seismogenic layer and the maximum length of faults; and

(2) the effective elastic plate thickness and the maximum width of basins,

but their observations are restricted to fault lengths and seismogenic layer thicknesses less than 30 km. The unusually deep (*ca.* 35 km) seismicity and long (greater than 50 km) border-fault segments in East Africa (see, for example, Ebinger *et al.* 1989; Jackson & Blenkinsop 1997) occur in relatively strong lithosphere (see, for example, Bechtel *et al.* 1987; Ebinger *et al.* 1991). Hayward & Ebinger (1996) noted a systematic decrease in the length and width of seismically active rift segments in the Afar Rift with decreasing effective elastic thickness, suggesting that the rheology of the upper continental lithosphere exerts a strong control on rift-basin geometry.

In this study, we report systematic variations in border-fault length and basin width within parts of the East African Rift system, which encompasses extensional segments of various ages (30 Ma to less than 2 Ma), progressive degrees of extension ($\beta < 1.1$ to $\beta > 2.0$), and those with and without any surface expression of volcanism (see, for example, Ebinger 1989; Hayward & Ebinger 1996; and figure 2). We then show that border-fault length and basin width in the East African, as well as the Aegean and Baikal, Rifts increase with the effective elastic plate thickness and seismogenic layer thickness, with implications for predictive models of rift basins and the rheology of continental lithosphere.

2. East African rift basins

The seismically and volcanically active rift systems of East Africa have developed atop two broad plateaux: the Afar Rift and Main Ethiopian Rift (MER) transect the 1000 km wide Ethiopian plateau; the Eastern and Western Rifts cut the 1300 km wide East African plateau (figure 2). The broad plateaux, their corresponding negative Bouguer gravity anomalies, the generally small degrees of extension, and the geochemistry and large volume of eruptive volcanic products are evidence for one or more mantle plumes beneath East Africa (see, for example, Mohr 1983; Ebinger *et al.* 1989; Marty *et al.* 1996). The Turkana depression between the Ethiopian and East African plateaux may be a topographic low between two discrete swells (Stewart & Rogers 1996), or the depression may be caused by isostatic compensation for crust thinned during Mesozoic and/or Palaeogene rifting (see, for example, Bosworth 1992; Hendrie *et al.* 1994).

The 21 mm a^{-1}, NE–SW-directed extension in the Red Sea, Gulf of Aden, and eastern Afar determined from geodetic studies (see, for example, Ruegg *et al.* 1993), changes to the much slower (3–8 mm a^{-1}) sub-E–W-directed extension in the MER (see, for example, Asfaw *et al.* 1992; and figure 2). The rate and direction of extension determined from the MER geodetic observations are consistent with current plate models and extension directions seen in earthquake focal mechanisms of teleseismic events (Jestin *et al.* 1994; Foster & Jackson 1998). Within the Eastern and Western rifts where extensional velocities are poorly constrained, well-determined focal mechanisms show predominantly dip-slip movement in directions nearly orthogonal to the approximately N–S-striking border faults (see, for example, Nyblade & Langston 1995; Foster & Jackson 1998).

Although the earliest record of rifting is buried by volcanic products in Afar, initial volcanism and faulting along the length of the Red Sea commenced at *ca.* 32 Ma

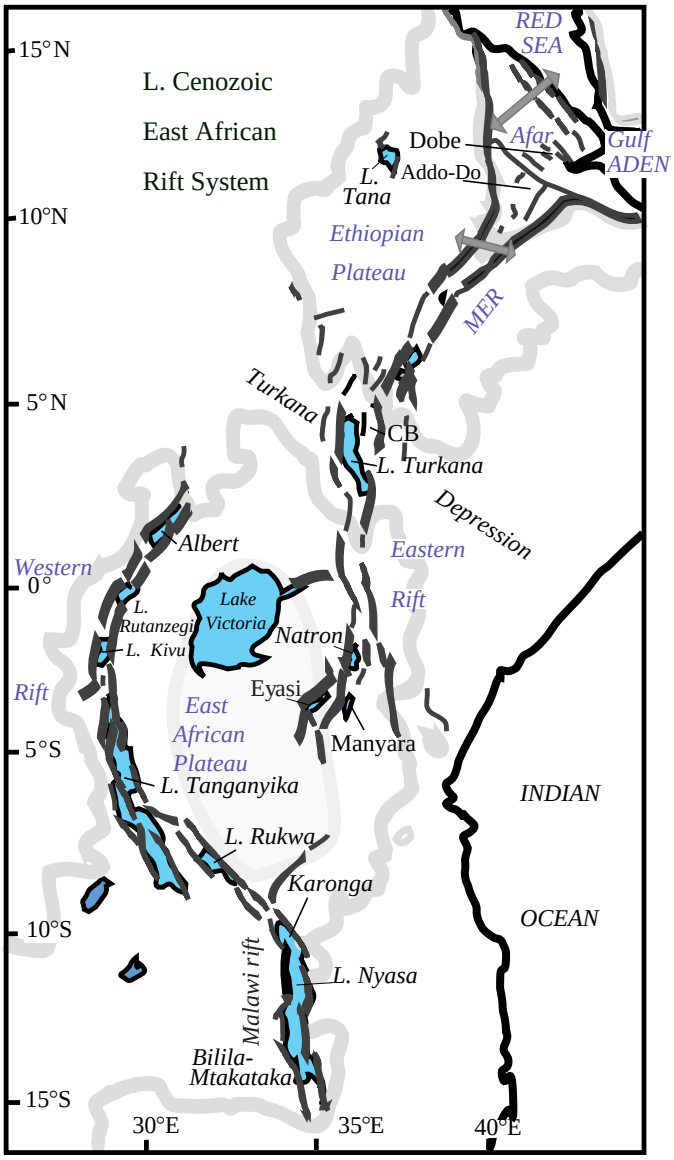

Figure 2. Summary tectonic map of the East African Rift system showing location of the Tanzanian craton and specific rift basins described in more detail in the text. Bold shaded lines enclose plateau elevations above 1000 m. Shaded arrows show extension direction in the Afar and Main Ethiopian rifts (MER). CB is Chew Bahir Basin.

(see, for example, Omar & Steckler 1996; Menzies *et al*. 1997), and extension in the Gulf of Aden had begun by 30 Ma (see, for example, Menzies *et al*. 1997). Sea-floor spreading has propagated into the easternmost Afar depression during the past 5 Ma (see, for example, Manighetti *et al*. 1998). Faulting and sedimentation began within the northern Eastern Rift and the Main Ethiopian Rift (MER) by *ca*. 20 Ma (see, for example, WoldeGabriel *et al*. 1990; Morley *et al*. 1992). Faulting and volcanism have

Table 1. *Comparison of continental rift segment properties*

(C is T_e estimate from coherence analyses, F is T_e estimate from forward modelling. See text for references to fault length, basin width and β-factor. Rift sectors shown on figure 2; MER is Main Ethiopian Rift; ER is Eastern Rift; WR is Western Rift; AG is Aegean Rift; CBK is Central Baikal Rift.)

rift sector	basin	width (km)	fault length (km)	T_e C (km)	T_e F (km)	T_{seis} (km)	β-factor
Afar	Dobe	12	34 ± 1	6[a]	5[a]	< 10[b]	< 1.5
Afar	Addo-Do	15	27 ± 1	6[a]	< 10[b]	< 1.5	
MER	Chew Bahir	38	65 ± 5	18[a]	*ca.* 15[b]	< 1.3	
ER	Natron	38	$67 + 2/-2$	24[e]	*ca.* 20[b]	< 1.1	
ER	Manyara	50	$82 + 10/-5$	24[e]	*ca.* 35[b]	< 1.1	
ER	Eyasi	47	$97 + 10/-5$	> 40[e]	*ca.* 35[b]	< 1.1	
WR	Albert	45	75+	30[c]	24[f]	*ca.* 20[b]	< 1.2
WR	Karonga	60	$120 + 10/-2$	35[a]	34[d]	*ca.* 35[g]	*ca.* 1.1
WR	Bil-Mtaka	65	100	35[c]	*ca.* 35[g]	< 1.1	
AG	Corinth	37	30 ± 5	10[h]	8[h]	< 15[h]	*ca.* 1.4
CBK	South Basin	65	$120 + 30/-5$	50[j]	40[k]	*ca.* 40[j]	< 1.2

Data sources for T_e and T_{seis} estimates:

[a]Hayward & Ebinger (1996); [b]Foster & Jackson (1998); [c]Ebinger *et al.* (1989); [d]Ebinger *et al.* (1991); [e]Ebinger *et al.* (1997); [f]Upcott *et al.* (1996); [g]Camelbeeck & Iranga (1996); [h]King (1998); [j]Petit (1996); [k]van der Beek (1997).

propagated southward in the Eastern and largely avolcanic Western Rifts during the past 12 Ma (see, for example, Ebinger *et al.* 1989; Foster *et al.* 1997; and figure 2). Crustal thickness estimates from seismic refraction and receiver function studies indicate thinning by a factor of two or more in northern Afar, but decreasing to a factor of less than 1.5 in the northern MER, and in the Eastern and Western Rifts (see, for example, Mechie *et al.* 1994; Last *et al.* 1997; and table 1).

East African Rift border faults have developed in metamorphic basement rocks ranging in age from Archaean to Pan-African (more than 500 Ma), as well as in flood basalt sequences of Oligocene–Recent age. Numerous researchers have noted that the East African extensional provinces formed along the margins of the Tanzanian craton within Proterozoic orogenic belts, and suggest that border-fault geometries are controlled by Precambrian upper crustal structures (see, for example, Wheeler & Karson 1989; Theunissen *et al.* 1996; and figure 2). Below, we evaluate the local relationship between Miocene–Recent East African border faults and pre-existing upper crustal structures to assess basement controls on border-fault geometry.

3. Rift segment dimensions

A brief summary of constraints on border-fault geometry, kinematics and seismicity patterns within East African Rift segments is provided below and in table 1. We use published cross-sections to illustrate the general form of East African basins and

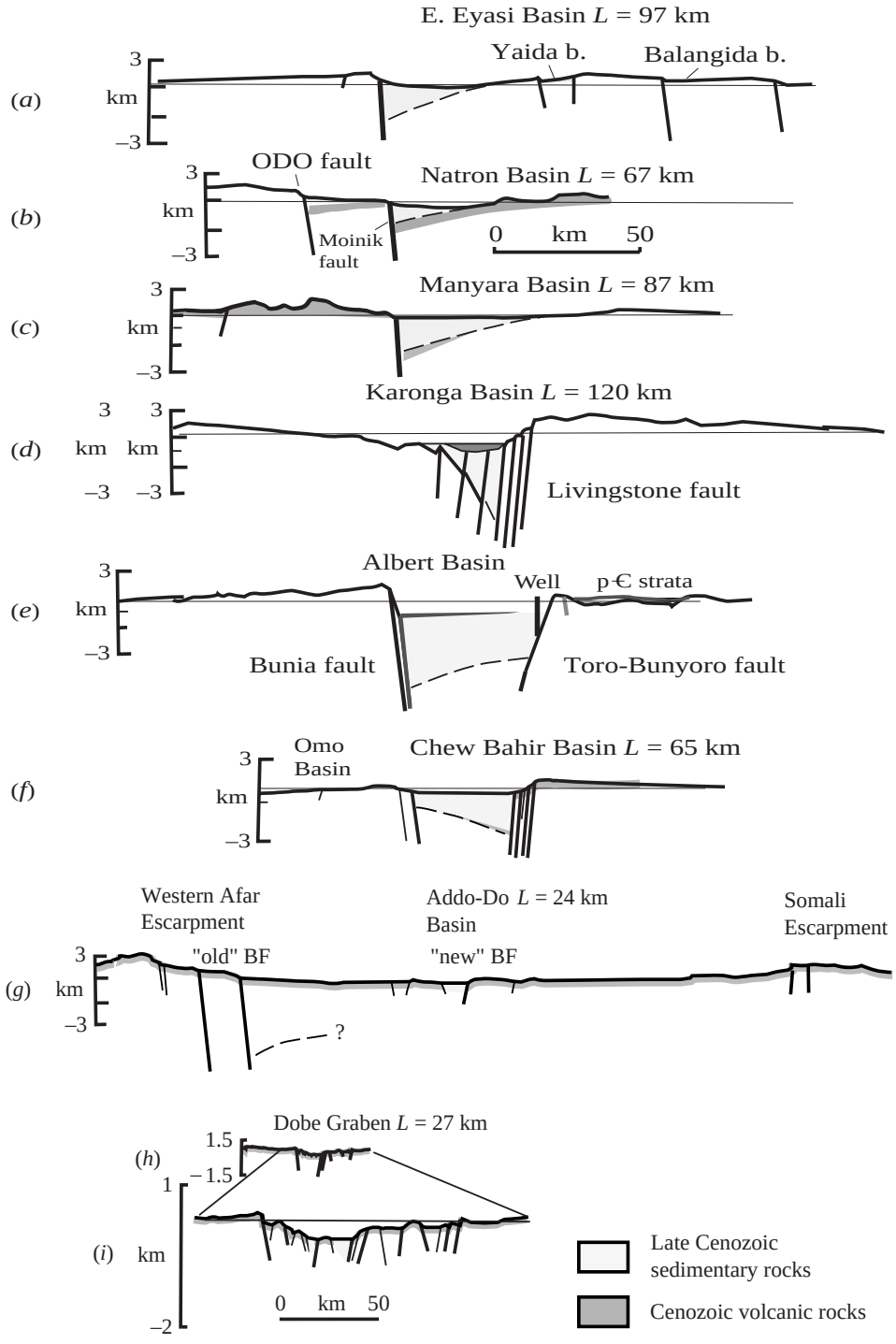

Figure 3. For description see opposite.

uplifted rift flanks, but subsurface data are insufficient to characterize the internal basin forms (figure 3). Basins are depressions bounded by one border-fault system that comprises one or more linked fault segments (see below), but the along-axis segmentation of basins may differ from that of border-fault segments, depending on the geometry of accommodation zones (see, for example, Trudgill & Cartwright 1994; Anders & Schlische 1994). Normal fault systems may propagate and eventually link to form a continuous border-fault system during the earliest stages of basin development, with the record of this along-axis propagation preserved in intrabasinal highs and relay-ramps (see, for example, Anders & Schlische 1994; Trudgill & Cartwright 1994). The border-fault systems bounding East African basins described below developed during the last 1–15 Ma, and some show signs of this propagation and linkage process.

A comparison of rift-basin cross-sections along the length of the East African Rift system shows the broad basins and uplifted flanks in the rifts that have developed in Archaean–Proterozoic lithosphere (figure 3). The breadth of the uplifted flank decreases with decreasing effective elastic thickness (see, for example, Weissel & Karner 1989; Ebinger *et al*. 1991), and we see that the breadth also decreases with fault length L, if we exclude areas of volcanic construction.

Descriptions are listed in an approximate evolutionary order, commencing with the youngest and least extended regions. Border faults have been mapped along their length in the field or in high resolution (less than 30 m) Landsat imagery (Ebinger 1989; Wheeler & Karson 1989; Hayward & Ebinger 1996; Jackson & Blenkinsop 1997; Upcott *et al*. 1996; Foster *et al*. 1997). Wherever possible, we report the lengths of other border faults within the same rift sector, and the relationship between metamorphic basement structures and Cenozoic faults. Estimates of maximum extension factor (β) estimated from seismic data and, more commonly, reconstructions of fault geometries are also listed for regional comparisons (table 1).

Fault segment length cannot be assessed without a definition of scale. Dawers & Anders (1995) show that continuous faults at one scale are in fact segmented. Lateral or en echelon offsets as small as 1–2 km across strike are known to halt earthquake ruptures (see, for example, Yielding 1985), and we use 2 km as the maximum offset allowed along a continuous fault segment (Foster 1997). Foster (1997) and LeTurdu *et al*. (1999) examined sharp bends in fault traces in the Eastern Rift, and found no offsets or changes in elevation of beds within the layered volcanic sequences forming the escarpment, indicating that faults were continuous through these bends.

There are several sources of error in our fault length measurements. First, the resolution of remote sensing imagery and topographic data make it difficult to determine the termination of fault segments where displacements approach zero. Given a low recurrence rate of major earthquakes in East Africa (see, for example, Ambraseys

Figure 3. Representative cross-sections of East African Rift basins shown in figure 2. Elevations are from 1:50 000 topography maps and gravity station heights. The top diagram of the Dobe graben (h) is shown at the same scale as the others, but (i) cross-section is a smaller scale in order to show details of the basin form. L is the length of the border fault (table 1). In (a) ODO is Ol Donyo Ogol Fault; MF is Moinik Fault. In (g) 'old BF' is the initial Oligo–Miocene Border Fault and 'new BF' is the Pliocene–Recent Border Fault. (a), (b), (c) from Foster *et al*. (1997), (d) from van der Beek *et al*. (1998); (e) from Upcott *et al*. (1996), (f) from Ebinger & Ibrahim (1994); (g), (h) and (i) from Hayward & Ebinger (1996). Note the decrease in the breadth of the uplifted rift flank with decreasing fault length (and effective elastic thickness, table 1).

1991*a*, *b*; Foster & Jackson 1998), alluvium and volcanic flows may cover the low relief tips of fault segments. A second source of error comes in the interactions with other faults, including intrabasinal and transfer faults (see, for example, Trudgill & Cartwright 1994; Anders & Schlische 1994). Therefore, we restrict our data-set to those border faults (comprising one or more fault segments) that are isolated and show clear terminations. Basin widths are measured relative to the mean elevation away from the uplifted rift flanks, as shown in figure 1*a* (figure 3, table 1).

Few historic earthquakes in East Africa have any known surface fault breaks to compare with border-fault lengths, but Jackson & Blenkinsop (1997) present evidence showing that the entire length of border faults can slip in a single earthquake. Although large earthquakes in East Africa are relatively infrequent, Ambraseys (1991*a*, *b*) reports two historic earthquakes of magnitude greater than 7.0 within the East African Rift.

(*a*) *Southern end of the Eastern Rift: Eyasi, Natron, Manyara Basins*

The southern end of the Eastern Rift is unique; faults have developed in the Tanzania craton (Archaean), rather than the Late Proterozoic orogenic belts ringing the craton (figures 2 and 4). Mantle xenoliths (see, for example, Dawson 1992) and tomographic models (Ritsema *et al*. 1998) indicate that the thermal lithosphere is thicker than 200 km beneath the craton, considerably more than the lithosphere beneath the Eastern Rift north of Lake Natron, which is less than 100 km thick (see, for example, Birt *et al*. 1997). There is no clear change in crustal thickness or velocity structure across the Archaean–Late Proterozoic surface contact (Last *et al*. 1997), and Archaean lithosphere may continue east beneath thin-skinned thrusts of the Pan-African orogenic belt.

The NE-striking Eyasi border fault is the largest fault within the Eastern Rift, and it cuts across the surface contact between Archaean and Pan-African (*ca*. 600 Ma) crust (figures 4 and 6*a*). This 47 km wide half-graben is partly filled by 2–3 km of sedimentary and volcanic strata as estimated from models of gravity and magnetic data (Ebinger *et al*. 1997). The Eyasi border fault developed at about 3 Ma (Foster *et al*. 1997).

The Natron Basin is a half graben bounded on its western margin by several long normal faults, the longest of which is the 67 km long, east-dipping Moinik Fault that cuts a parallel-bedded sequence of basalts, constraining the age of the fault to less than 1 Ma (see Foster *et al*. 1997; and figure 3*b*). The *ca*. 85 km long Ol Donyo Ogol Fault lies *ca*. 15 km west of the Moinik Fault, and this apparently inactive fault marked the margin of an earlier (Mid-Pliocene?) basin (see, for example, Foster *et al*. 1997).

The western margin of the *ca*. 50 km wide, *ca*. 100 km long Manyara Basin is bounded by seismically active high-angle normal faults, the longest of which is at least 82 km in length (figure 3*c*). The northern part of this segment cuts the less than 1 Ma flood basalt sequence, whereas its southern part cuts Pan-African basement, making it difficult to assess its age and continuity there. South and west of the Manyara Basin, seismically active, greater than 40 km long, normal faults are morphologically the youngest faults in the region (see, for example, Balangida Fault, figure 4 and Foster *et al*. 1997). They may mark the initial stage of development of long border faults.

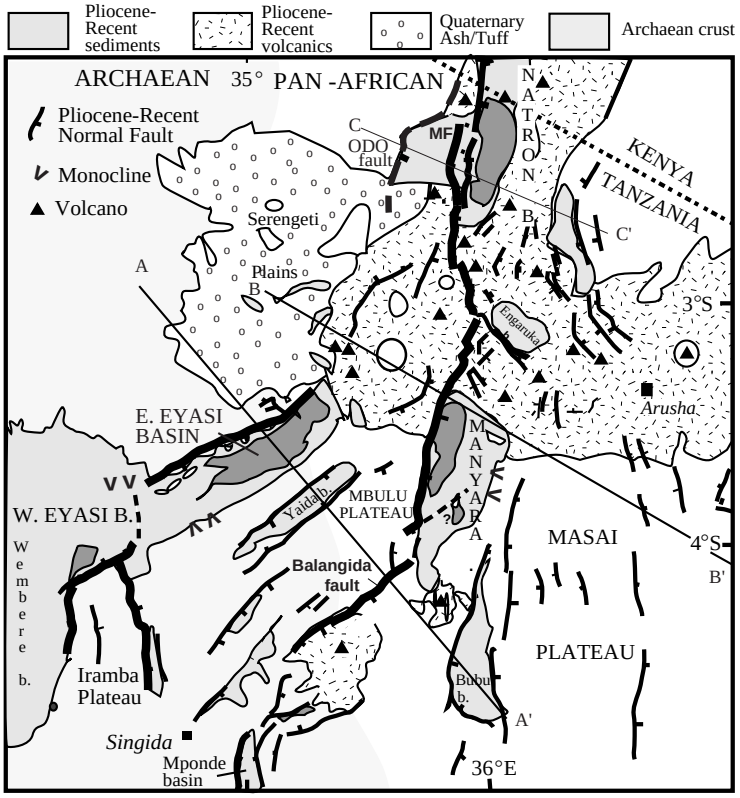

Figure 4. Summary geological map of the Eyasi–Natron–Manyara Basins at the southern end of the Eastern Rift, illustrating the predominance of long normal faults and wide basins. A–A′, B–B′ and C–C′ are lines of cross-sections shown in figure 3. Elevations are from 1:50 000 topography maps and gravity station heights. ODO is Ol Donyo Ogol Fault.

Although there is a parallelism between rift faults and N–S to NE–SW striking Pan-African structures at the regional scale, recumbent Pan-African folds are thin skinned (Shackleton 1993) and are cross-cut by steeply dipping Late Cenozoic normal faults. Basement foliations and shear zones within the Pan-African belt are locally highly variable, and there is little correlation between basement structures and faults along the eastern margins of the Natron and Manyara Basins (Foster *et al*. 1997). Precambrian diabase dykes are subparallel or coincident with segments of the Eyasi Border Fault, suggesting that some parts of the Eyasi fault zone reoccupy basement shear zones.

Earthquakes detected both teleseismically (Nyblade & Langston 1995; Foster & Jackson 1998) and locally occur throughout the 35 km thick crust beneath this region, which is the most active seismically in East Africa (see, for example, Nyblade *et al*. 1996).

(*b*) *Western Rift: Bilila–Mtakataka, Karonga and Albert Basins*

The *ca*. 100 km long Bilila–Mtakataka Fault bounds the western side of the southern Malawi Rift where less than 1 km of sedimentary strata have accumulated (see

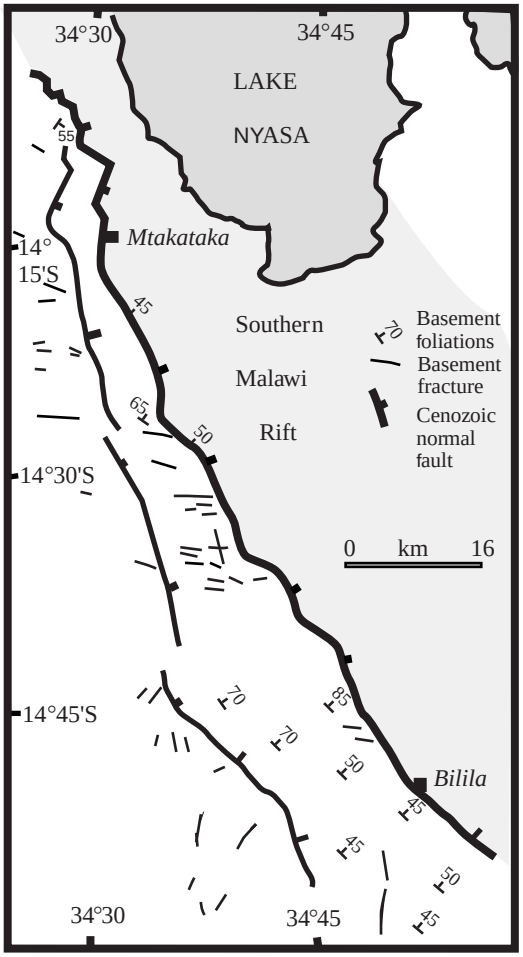

Figure 5. Summary structural map of the Bilila–Mtakataka border-fault segment showing the geometry of the *ca.* 100 km long border fault and representative strikes and dips of Late Proterozoic basement foliations and fractures (from Jackson & Blenkinsop 1997). Shaded area shows the approximate extent of the sedimentary basin at the foot of the border fault.

Jackson & Blenkinsop 1997; and figure 5). The dip of the fault plane is generally greater than 60° NE (Jackson & Blenkinsop 1997). Although there is a strong correlation between the strike of this fault and Late Proterozoic basement foliations at the regional scale, foliations show more complex deviations in strike and dip at the outcrop scale (Jackson & Blenkinsop 1997; and figure 5). Some segments of the fault also show parallelism with sub-vertical WNW-striking fractures (figure 5).

An earthquake at a depth of 32 ± 5 km occurred immediately to the north of the fault in 1989, and field observations suggest that most or all of the 100 km long Bilila–Mtakataka fault slipped in a Late Quaternary earthquake (Jackson & Blenkinsop 1993, 1997). Jackson & Blenkinsop (1997) estimate that a Mw 8.0 earthquake would be required to cause slip along this fault, which is much larger in magnitude than typical continental rift events. Normal faulting earthquakes of comparable mag-

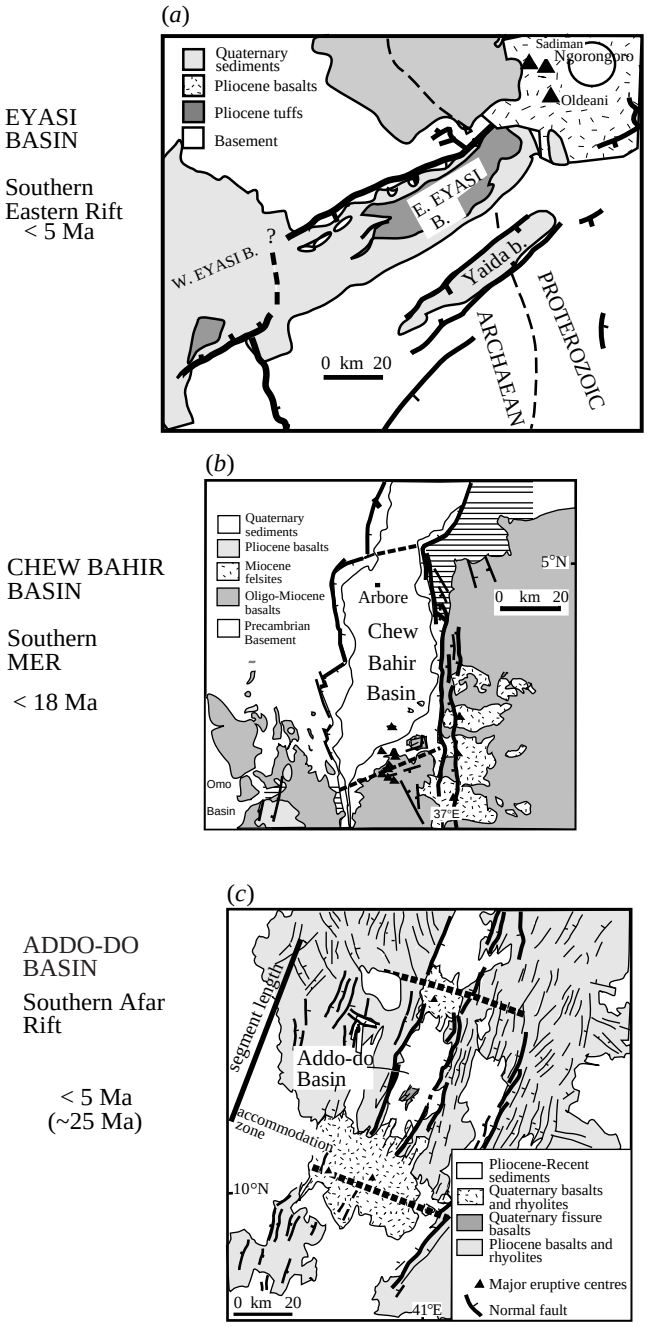

Figure 6. Fault patterns within three representative East African Rift basins showing the change in scale of the border faults and basin dimensions as elastic plate thickness decreases, as estimated from seismogenic (T_{seis}) and effective elastic (T_{e}) thickness. Approximate age of faults indicated to the left of diagrams. All diagrams at the same scale. The less than 5 Ma old Addo-do Basin developed in the hangingwall to an *ca.* 20 Ma old western Afar border fault (figure 3*g*). Note the increase in number and displacement of intrabasinal faults as T_{e} decreases.

nitude, however, have occurred in oceanic lithosphere seaward of trenches, causing rupture at depths of 40 km or more (see, for example, Kikuchi & Kanamori 1995).

The *ca.* 60 km wide Karonga Basin at the northern end of the Malawi Rift is bounded by the 120 km long Livingstone Fault. The northern part of the border fault had developed by *ca.* 8 Ma (Ebinger *et al.* 1991). Depth to pre-rift basement is greater than 4 km at the base of the Livingstone Fault, constraining throw along the fault to greater than 6 km (Wheeler & Karson 1989; van der Beek *et al.* 1998; and figure 3*d*). Only minor basement-involved faults occur across the basin, with nearly all of the less than 10 km crustal extension accommodated along the Livingstone Fault (Wheeler & Karson 1989; Ebinger *et al.* 1991; and figure 3*d*).

The central and southern parts of the Livingstone Border Fault are exceptional in East Africa, in that they reoccupy Precambrian ductile shear zones (Wheeler & Karson 1989; Theunissen *et al.* 1996). Here, brittle fractures and pseudo-tachylite developed within the most highly strained parts of a steeply dipping Late Proterozoic shear zone (Wheeler & Karson 1989).

Seismicity patterns recorded on local networks show a distribution throughout the *ca.* 40 km thick crust (Camelbeeck & Iranga 1996; Zhao *et al.* 1997). Teleseismic data show centroid depths of *ca.* 25 km for two earthquakes located to the north of the Karonga Basin, but no teleseismic events have been recorded in this basin (Foster & Jackson 1998). Seismically active, long (more than 120 km) normal faults north of the Karonga Basin are excluded from the database because at least parts of these border faults developed during a Permo-Triassic (Karoo) rifting episode, and they show evidence for oblique-slip movement during one or both rifting episodes (see, for example, Delvaux *et al.* 1998). One of these long faults, the 170 km long Kanda Fault, may have been the site of the 1910 Rukwa earthquake, the largest recorded in Africa (Ambraseys 1991*a*; Delvaux *et al.* 1998).

The northwestward-tilted North Albert Basin is bounded to its northwest by the 75 km long Bunia fault (Upcott *et al.* 1996; and figure 3*e*). The Bunia segment could be up to 20 km longer, but access to the southern portions of the fault in Zaire was impossible. Another long fault with smaller throw, the 58 km long Toro–Bunyoro Fault, bounds the opposite side of the basin, and its subsurface geometry is well constrained by borehole, gravity and magnetic data (Upcott *et al.* 1996; and figure 3*e*). No eruptive volcanic centres occur along the border faults, but a few Neogene carbonatitic vents are located south of the rift (see, for example, Upcott *et al.* 1996).

Foliations within Archaean to Early Proterozoic metamorphic basement strike N–S to NE–SW throughout the area, but dips are highly variable. Bends in the Toro–Bunyoro Fault near its southern termination cross-cut these basement structures, arguing against reactivation of pre-existing upper crustal structures.

A 1966 dip-slip earthquake southwest of Lake Albert led to the development of a 20 km long fault scarp with 1.8 m displacement (Ambraseys & Adams 1986). Foster & Jackson (1998) show centroid depths of less than 20 km for earthquakes in the Albert Basin and Ruwenzori horst to its south.

(*c*) *Main Ethiopian Rift: Chew Bahir Basin*

The southern Main Ethiopian Rift (MER) developed in Pan-African lithosphere that was affected by rifting in Cretaceous and probably Palaeogene time (see, for

example, Bosworth 1992; Hendrie *et al*. 1994). Thus, geothermal gradients were probably higher than in adjacent rift sectors (Hendrie *et al*. 1994), and the initial crustal thickness may have been less than the 35–40 km found in most of East Africa (see, for example, Mechie *et al*. 1994; Last *et al*. 1997).

Miocene basalts along the eastern margin of the Chew Bahir Basin are offset more than 1000 m by displacement along the *ca*. 65 km long border fault (figures 3*f* and 6*b*). Its southern termination can only be estimated to within 5 km because it is covered by landslide deposits of felsic ignimbrites (see, for example, Davidson 1983). The 40 mGal negative Bouguer anomaly observed across the Chew Bahir Basin can be explained by 1–2 km of sedimentary to volcanic rocks within the basin (see Ebinger & Ibrahim 1994; and figure 3*f*).

There is little evidence for reactivation of generally low angle gneissic foliations in metamorphic basement or Mesozoic normal faults, where basement is exposed (Davidson 1983). Several earthquakes were detected teleseismically in the region, and aftershocks were recorded on a local network (Asfaw 1992). Focal depths of 9 and 14 km were determined from centroid moment tensor inversions for two earthquakes with dip-slip mechanisms orthogonal to border faults, but the epicentral locations are too inaccurate to determine if the border faults are still active (Foster & Jackson 1998).

(*d*) *Afar: Addo-do, Dobe Basins*

Morphological evidence from the Western Fault line escarpment to the greater than 250 km wide Afar depression suggests that the short Addo-do and Dobe segments are young, and developed within the hanging wall to originally longer border faults (see Hayward & Ebinger 1996; and figure 3*g*). The Late Oligocene western Afar escarpment has undergone considerable erosion, but drainage patterns into the Afar and away from the rift along the westward-tilted uplifted flank indicate that Early Miocene fault lengths were more than 50 km (see, for example, Weissel *et al*. 1995). The centroid depth for an earthquake located near or along the escarpment is *ca*. 7 km (Foster & Jackson 1998), but there is little evidence in the field or in remote sensing imagery for active faulting along the eroded escarpment. Thus, we believe that active extension within the highly extended Afar Rift occurs along the short fault segments in the central Afar depression, and that long faults along the western escarpment are inactive (figure 3*a*).

Pliocene–Recent Rift basins in the central Afar depression developed in thinned lithosphere, and total extension across these basins is the cumulative extension since rift initiation. Extension estimates in the 'new' basins of Afar shown in table 1, however, represent extension from the Pliocene–Recent stage, when the 'new' along-axis segmentation developed, to keep these estimates consistent with others shown in table 1.

Faults bounding the Addo-do Basin cut Pliocene–Pleistocene flood basalts, and Quaternary eruptive centres occur near the tips of border-fault segments (e.g. figure 6*c*). The largest normal fault is 27 km long, whereas the mean length of fault segments is 5 km, with fault length decreasing toward the Central Basin (see Hayward 1996; and figures 3 and 6*c*).

Strain in the 15 km wide Dobe graben is accommodated along border and intrabasinal faults that cut Quaternary basalt flows, producing stratal dips of 30–35° (see

Hayward & Ebinger 1996; and figure 3*i*). The longest fault in the population of 273 faults measured from Landsat and space shuttle imagery is 35 km, the master fault to the Addo-do Basin, whereas the mean length of faults is only 5 km (Hayward 1996).

Nowhere is metamorphic basement exposed in or near the Addo-do or Dobe Basins to assess basement controls on Pliocene–Recent faults. A large earthquake and 10 teleseismically detected aftershocks in 1989 were located along border faults bounding the Dobe Basin (Sigmundsson 1992). Braunmiller & Nabelek (1990) determine depths of 4–7 km for these earthquakes.

(*e*) *Summary*

Although the data-set is small, consistent patterns are seen along the length of the East African Rift system, regardless of proximity to, or volume of, magmatism (table 1, figure 3). The border fault and basin scales also appear to be independent of the age, metamorphic grade, or orientation of the Precambrian basement in which the rift system has developed. Long border-fault segments bounding broad basins with broad uplifted flanks characterize the young basins with small degrees of extension that developed in cratonic lithosphere. Basins within the southern MER (e.g. Chew Bahir), where lithosphere was heated and stretched in Cretaceous time, show similar patterns, but fault segments are shorter and basin widths narrower. Segments within the northern MER (e.g. Addo-do) and southern Afar (Dobe) preserve the 'long border-fault phase' along the eroded escarpments bounding the rift, but a new, shorter segmentation has developed within the highly extended and intruded central rift floor (see, for example, Hayward & Ebinger 1996; and figures 3*g* and 6*c*).

The consistent patterns in border-fault geometry within a number of Precambrian and Archaean terrains with different structural trends argues against a basement control on rift dimensions. From a regional analysis of border faults by Ring (1994), border-fault segments may reactivate pre-existing basement structures, particularly cataclastic strike-slip shear zones, if these structures are orientated within *ca.* 30° of the extension direction, similar to laboratory studies. Thus, the orientation of a particular border-fault segment may be sub-parallel to pre-existing upper crustal structure where the stress field is favourably orientated (e.g. Eyasi Basin), but the actual fault lengths are more closely linked to the earthquake rupture process (see, for example, Das & Scholz 1983). Some parts of the longest faults (Bilila–Mtakataka, Eyasi, Karonga), however, show reactivation of basement shear zones or pre-rift dykes, suggesting that pre-existing fractures enhance fault development.

4. Correlation with effective elastic and seismogenic thicknesses

The lithospheric response to the faulting process is two-fold: there is a co-seismic deformation of the lithosphere that occurs over periods of years; and a flexural isostatic response over periods greater than 10^4–10^5 years (see, for example, Stein & Barrientos 1985; Weissel & Karner 1989). The longer-term isostatic response, as well as erosion and deposition, modifies the co-seismic displacement field. Direct models of the co-seismic and isostatic response of the continental lithosphere, however, are complicated by our poor understanding of its rheology and composition (see, for example, Ma & Kusznir 1994; Burov & Diament 1995). If this rheology can be

represented by an equivalent elastic plate (effective elastic thickness, T_e), we can predict the response of lithosphere with different thicknesses to faulting processes, and compare models with observations. Clearly, though, more complicated models are needed to explain the detailed stratigraphy within any discrete rift-basin segment (see, for example, Contreras *et al*. 1997).

Scholz (1988) argues that the thickness of the seismogenic layer (T_{seis}) is controlled by the depth-dependent frictional behaviour of the upper crust, which in turn depends on geothermal gradient and crustal composition. Effective elastic thickness (T_e) does not usually correspond to any depth horizon or the actual thickness of any particular lithospheric layer, but it is believed to represent the combined effective strength of the crust and upper mantle, which varies with composition, strain rate and geothermal gradient (see, for example, Burov & Diament 1995). If the upper mantle of continental lithosphere is weak, the seismogenic layer may be a proxy for effective elastic thickness (see, for example, McKenzie & Fairhead 1997). Considering these properties, the duration of heating from below from a mantle plume and/or stretching, as well as the volume of magmatic material accreted to the lithosphere, will modify elastic thickness, as measured by variations in T_e and T_{seis}.

T_e within rifts has been estimated from forward models of topography and gravity anomaly profiles, and from two-dimensional inverse models of the coherence between gravity anomalies and topography (see, for example, Weissel & Karner 1989; McKenzie & Fairhead 1997). It is commonly assumed that these rift gravity anomalies arise from warpings of surface and Moho after faulting and isostatic compensation. Forward models require constraints on the density of infilling material, β-factor (amount of extension), and depth to detachment (necking depth). If models are required to fit both gravity anomalies and topography, T_e is usually well bracketed (see, for example, Weissel & Karner 1989; Ebinger *et al*. 1991). The Bouguer coherence method is the most commonly used inversion technique, and it is a spectral method that may be biased to stronger values due to the spatial averaging of data from rift basins and flanks (see, for example, Ebinger *et al*. 1989; McKenzie & Fairhead 1997). We report both estimates wherever possible (table 1).

Table 1 and figure 6 show that seismicity extends throughout the crust in the relatively strong, weakly magmatic or amagmatic, mildly extended rift segments, but that it decreases to less than 10 km in the central Afar depression. Clearly, the period of seismicity observations is extremely short, but these south to north variations are mirrored in the variations in T_e (table 1). Estimates of effective elastic plate thickness based on the coherence between the topography and Bouguer gravity as a function of wavelength vary from *ca.* 6 to greater than 40 km, with the lowest values found in the highly attenuated lithosphere of Afar.

McKenzie & Fairhead (1997) present an alternative approach to T_e estimations and their interpretations. A detailed comparison of techniques is outside the scope of this study, but we provide a summary of arguments presented in King (1998). McKenzie & Fairhead (1997) use the free-air admittance method to obtain T_e estimates of *ca.* 15 km for the Eastern Rift, considerably smaller than estimates of greater than 30 km obtained by Ebinger *et al*. (1989, 1997). They assume that topographic relief is compensated within the crust, implying that the upper mantle has no long-term strength. The more traditional Bouguer coherence analysis, however, considers the gravity anomaly to be the sum of surface and subsurface (approximately Moho) density distributions, or topographic relief, at the base of the continental crust, as

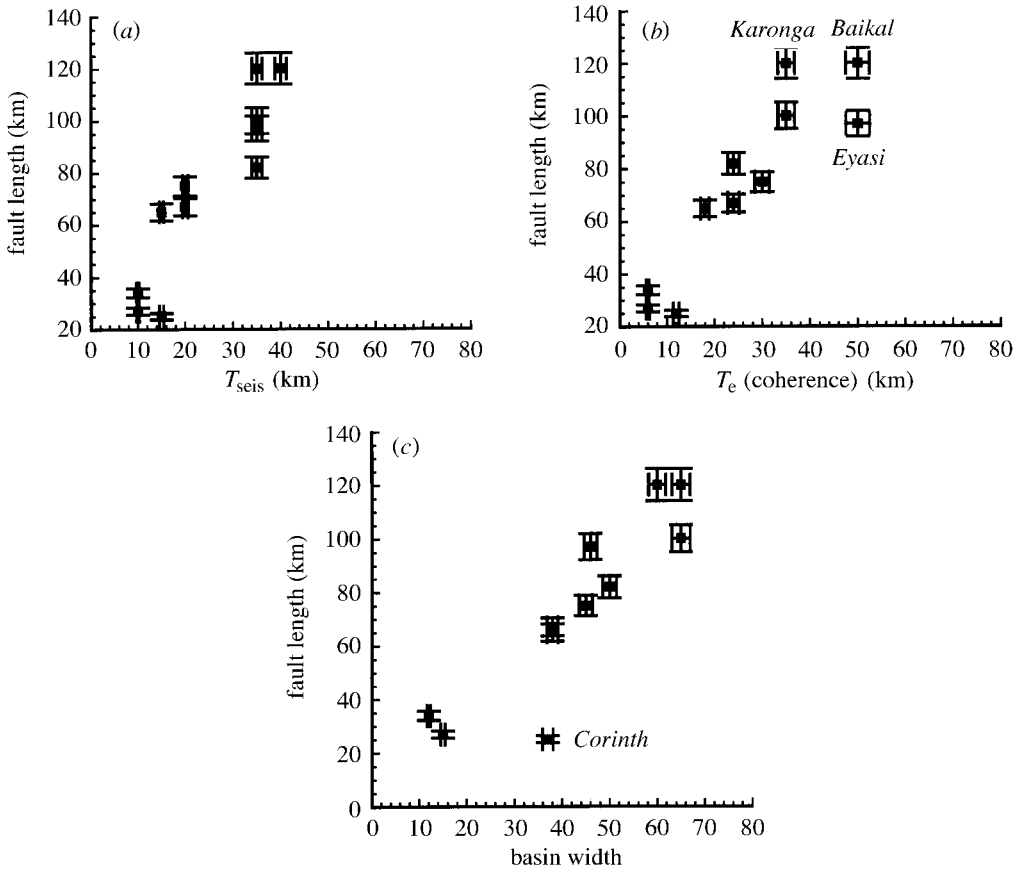

Figure 7. Comparison of border-fault length and (*a*) seismogenic layer thickness (T_{seis}); (*b*) effective elastic thickness (T_e); and (*c*) basin width using observations listed in table 1. All of the diagrams show a linear increase in fault length as T_e, T_{seis} and basin width increase. Note that β is higher in the Corinth Basins.

imaged in seismic data (Ebinger *et al*. 1989). In both the free-air and Bouguer coherence techniques, sub-lithospheric density contrasts with length-scales of *ca.* 1000 km (dynamic contributions) may lead to spectral aliasing (see, for example, McKenzie & Fairhead 1997). Forward model estimates from several East African basins support the Bouguer coherence results (table 1), and we use the Bouguer coherence estimates as a comparative base throughout this study.

Figure 7 summarizes the correlations between border-fault segment length and T_e and T_{seis}, respectively. Both figure 7*a* and 7*b* show a linear increase in border-fault segment length with increasing thickness of the elastic lithosphere, as estimated by T_e and T_{seis}, respectively. The comparison of basin width and fault length also shows an apparent linear trend, but this relation probably holds only for basins with small extensional strains. Weissel & Karner (1989) model progressive stages of basin development at constant T_e, and show that basin width increases with stretching factor, β. The comparatively greater width for T_e or fault length (L) seen in the Gulf of Corinth outlier (table 1, figure 7*c*), could indicate that intrabasinal faults

accommodate significant extension, or reflect the shift in the location of border faults with time (Ori 1989).

5. Discussion

If our relationships are correct, we should see similar fault length versus elastic thickness patterns in other rifts. Extensional basins within the Baikal and the Aegean Rifts should represent the two end-members seen in East Africa: thick stronger lithosphere of the Eyasi Basin compared to thin weaker lithosphere of the Addo-do Basin.

The Baikal Rift developed within and along the margin of the Siberian craton, where geothermal gradients are low, seismicity occurs throughout the crust (Deverchere *et al*. 1991; Petit 1996), and estimates of effective elastic plate thickness from Bouguer coherence analyses and forward models are 30–50 km (Diament & Kogan 1990; Ruppel *et al*. 1993; van der Beek 1997). Seismicity data indicate that extension direction varies along the length of the Baikal Rift, and this variability may contribute to its along-axis segmentation (Petit 1996). The broad Central Basin of Lake Baikal, which contains *ca.* 7 km of sediments and water, is bordered to its northwest by the more than 120 km long Primorskiy Fault, which was delineated from Landsat imagery calibrated by field studies (Agar & Klitgord 1997). The subparallel synthetic *ca.* 150 km long Morskiy fault defines the deep lake basin (see, for example, Agar & Klitgord 1995), but the continuity of this sub-lacustrine fault cannot be evaluated in the same manner as other border faults used in this study. Antithetic normal faults on the opposite side of the Central Basin show considerably smaller throws and flank uplift, producing a faulted half graben cross-sectional morphology (Petit 1996). The dimensions of the Central Baikal Basin and its location along the margin of Archaean craton are similar to the tectonic characteristics of the Karonga and Eyasi Basins of East Africa (table 1, figure 7).

Extensional basins within the Aegean region developed over the past 20 Ma in relatively hot lithosphere of a collapsing orogenic belt (see, for example, Roberts & Jackson 1991). Discrete basins within the Corinth Rift contain *ca.* 3 km of sedimentary strata, and flanking uplifts rise more than 1000 m above the surrounding topography (King 1998; A. Hirn, personal communication). Border-fault lengths of 25–30 km within the Corinth and Evvia Rifts have been identified using spatial variations in fault displacements and kinematic indicators detected in the field and remote sensing imagery (see Roberts & Jackson 1991; and table 1). Seismogenic layer thickness determined from teleseismic and local arrays is 10–15 km (see, for example, Roberts & Jackson 1991). T_e estimates are less than 15 km from the coherence model, and less than 10 km from forward modelling (see King 1998; and table 1).

Are these values of T_e and T_{seis} consistent and compatible with independent constraints on faulting processes and lithospheric rheology? The deep seismicity and seismic velocities seen in the southernmost Eastern Rift and central Baikal Rifts, which developed in Archaean lithosphere, suggest that the lower crust here has a more mafic bulk composition (Nyblade & Langston 1995; Foster & Jackson 1998). The high strength and deep seismicity are consistent with the low geothermal gradients found in the southern part of the rift system (see, for example, Nyblade *et al*. 1990). In the Eyasi–Natron–Manyara Rift Basins of the Eastern Rift, there is no clear evidence for lateral variations in crust and upper mantle velocity structure or thickness across the Tanzania Craton–Pan-African orogenic belt boundary (Last *et*

al. 1997), suggesting that the deep seismicity within the Tanzanian craton primarily results from low geothermal gradients, rather than compositional changes (Foster *et al*. 1997).

Are T_e and T_{seis} measuring similar lithospheric properties, and what can we infer from their spatial variability? We can gain some information from numerical and analogue models. Forsyth (1992) estimates the stress required to cause a given amount of extension in a finite-strength lithosphere. Expanding on these relations, Hayward (1996) and Scholz & Contreras (1998) show that normal fault length and displacement increase with increasing T_e. Models of seismicity data indicate that the maximum fault rupture length scales with the thickness of the strong layer(s) within the deforming media (Das & Scholz 1983). The two- and three-dimensional numerical models of Gupta & Scholz (1998) suggest that elastic plate models can explain many aspects of small-scale extensional fault arrays without requiring complicated viscoelastic models (see, for example, Burov & Diament 1995; Petit 1996). Their results may be applicable at the scale of basin-bounding faults (10^0–10^2 km) (Schlische *et al*. 1996), since the scaling relationships are similar (Gupta & Scholz 1998).

Comparing T_e and T_{seis}, one could argue that the equivalent or slightly higher T_e estimates for a given border-fault length suggest that the continental mantle lithosphere also deforms elastically and is relatively strong. Unfortunately, it is the higher estimates of T_e determined from coherence studies that are subject to the largest errors, owing to data coverage and spectral averaging (Ebinger *et al*. 1989; McKenzie & Fairhead 1997). Forward models of basin and flank morphology provide T_e estimates that are 2–20% less than Bouguer coherence results that are probably biased to higher values, making T_e and T_{seis} values roughly equivalent within the errors of our observations (table 1).

Clearly, other processes will influence the border-fault length relations described in this paper, but we consider these to be second-order effects. Probably the most obvious influence is that of pre-rift basement fabrics and structures. The longest border faults in our database have strikes that are sub-parallel to pre-existing shear zones and dykes within metamorphic basement (e.g. Eyasi, Bilila–Mtakataka), and these zones of weakness may allow individual earthquakes to propagate a greater distance for the same seismogenic layer thickness (see, for example, Kostrov & Das 1988). Thus, these border faults may be anomalously long due to the combined effects of favourably orientated cracks, as well as a thick elastic lithosphere. Further consideration of these factors requires a larger database of basin dimensions, and better understanding of continental lithospheric rheology.

The consistent correlations between T_e or T_{seis} and border-fault length suggest that measurements of fault length distributions and geomorphology can be used to predict initial rift-basin lengths and widths, as well as the spacing between accommodation zones, in active rift zones. We would expect that both T_e and T_{seis} will change after rifting has ceased, but the border-fault length can still be used to predict the general basin width and tectonic setting.

6. Conclusions

Tectonically active continental rift basins are bounded by long border-fault systems that control the breadth and length of basins, the form of their uplifted flanks, and, indirectly, depositional patterns within basins. Our comparison of border-fault

dimensions in the East African, Baikal and Aegean Rifts show that long (greater than 80 km) border-fault segments bound deep broad rift basins that develop in cold thick lithosphere (Western and Eastern Rifts, Baikal); short (less than 30 km) border faults bound narrow basins within initially weak lithosphere (Aegean), or develop as a new segmentation within highly stretched and intruded lithosphere (Afar). The less than 30 km long, *ca.* 20 km wide rift segments in the Afar Rift overprint an older, longer rift segmentation preserved in eroded escarpments bounding the western margin of the Afar depression.

Border-fault length shows a linear increase with seismogenic layer thickness (T_{seis}) and with effective elastic thickness (T_{e}), both comparative measures of elastic plate thickness. These patterns observed within the East African Rift system, as well as the Baikal and Aegean Rifts, indicate that the fault and flexural response of the continental lithosphere to rifting processes is largely controlled by the elastic lithosphere. Further studies in other active continental rifts worldwide, however, are needed to extract information on the complicated rheology of the continental lithosphere from variations in fault length, T_{e}, and T_{seis}. Our results suggest that we can assess the form of rift basins and flanks and tectonic setting during the syn-rift stage using measurements of border-fault length, improving predictive models of rift-basin development.

The work of A.F. and J.J. was sponsored by grants from Shell and Amerada Hess. A.F. was supported by NERC grant GR9/997A, N.H. by NERC grant GR9/496A. C.E. was, in part, supported by a grant from Hunt United Exploration. Reviews by P. Cowie, R. Whitmarsh and an anonymous reviewer, and discussions with T. King, D. McKenzie and C. Petit improved this manuscript.

References

Agar, S. & Klitgord, K. 1995 Rift flank segmentation, basin initiation, and propagation: a neotectonic example from Lake Baikal. *J. Geol. Soc. Lond.* **152**, 849–860.

Ambraseys, N. 1991*a* The Rukwa earthquake of 13 December, 1910 in East Africa. *Terra Nova* **3**, 203–208.

Ambraseys, N. 1991*b* Earthquake hazard in the Kenya Rift: the Sabukia earthquake of 13 December 1910. *Geophys. J. Internat.* **3**, 203–208.

Ambraseys, N. & Adams, R. 1986 Seismicity of the Sudan. *Bull. Seism. Soc. Am.* **76**, 483–493.

Anders, M. & Schlische, R. 1994 Overlapping faults, intrabasin highs, and the growth of normal faults. *J. Geol.* **102**, 165–180.

Asfaw, L. M. 1992 Implication of shear deformation and earthquake distribution in the East African Rift between 4° N and 6° N. *J. African Earth Sci.* **10**, 745–751.

Asfaw, L. M., Bilham, R., Jackson, M. & Mohr, P. 1992 Recent inactivity in the African Rift. *Nature* **357**, 457.

Bechtel, T., Forsyth, D. & Swain, C. 1987 Mechanisms of isostatic compensation in the vicinity of the East African Rift, Kenya. *Geophys. J. R. Astr. Soc.* **90**, 445–465.

Birt, C., Maguire, P. K. H., Khan, M. A. & Thybo, A. 1997 A combined interpretation of the KRISP '94 seismic and gravity data: evidence for a mantle plume beneath the East African plateau. *Tectonophys.* **278**, 211–242.

Bosworth, W. 1992 Mesozoic and Tertiary rifting in East Africa. *Tectonophys.* **209**, 115–137.

Braunmiller, J. & Nabelek, J. 1990 The 1989 Ethiopia earthquake sequence. *Eos* **71**, 1480.

Burov, E. & Diament, M. 1995 The effective elastic plate thickness (T_{e}) of continental lithosphere: what does it mean? *J. Geophys. Res.* **100**, 3905–3927

Camelbeeck, T. & Iranga, M. D. 1996 Deep crustal earthquakes and active faults along the Rukwa trough, eastern Africa. *Geophys. J. Int.* **124**, 612–630.

Contreras, J., Scholz, C. & King, G. C. P. 1997 A model of rift basin evolution constrained by first-order stratigraphic observations. *J. Geophys. Res.* **102**, 7673–7690.

Das, S. & Scholz, C. H. 1983 Why large earthquakes do not nucleate at shallow depths. *Nature* **305**, 145–148.

Davidson, A. (compiler) 1983 The Omo River Project. Bulletin 2, Ethiopian Institute Geological Survey.

Dawers, N. & Anders, M. 1995 Displacement-length scaling and fault linkage. *J. Struct. Geol.* **17**, 604–614.

Dawson, B. 1992 Neogene tectonics and volcanicity in the north Tanzania sector of the Gregory Rift Valley: contrasts with the Kenya sector. *Tectonophys.* **204**, 81–92.

Delvaux, D., Kervyn, F., Vittori, E., Kajara, R. & Kilembe, E. 1998 Late Quaternary tectonic activity and lake level change in the Rukwa Rift. *J. African Earth Sci.* **26**, 397–421.

Deverchere, J., Houdry, F. & Diament, M. 1991 Evidence for a seismogenic mantle and lower crust in the Baikal Rift. *Geophys. Res. Lett.* **18**, 1099–1102.

Diament, M. & Kogan, M. 1990 Long wavelength gravity anomalies over the Baikal Rift and geodynamic implications. *Geophys. Res. Lett.* **17**, 1977–1980.

Ebinger, C. 1989 Tectonic development of the western branch of the East African Rift system. *Geol. Soc. Am. Bull.* **101**, 885–903.

Ebinger, C. & Ibrahim, A. 1994 Multiple episodes of rifting in Central and East Africa: a re-evaluation of gravity data. *Geol. Rundsch.* **83**, 689–702.

Ebinger, C., Bechtel, T., Forsyth, D. & Bowin, C. 1989 Effective elastic plate thickness beneath the East African and Afar plateaux, and isostatic compensation for the uplifts. *J. Geophys. Res.* **94**, 2893–2901.

Ebinger, C., Karner, G. & Weissel, J. 1991 Mechanical strength of extended continental lithosphere: constraints from the Western Rift system, Africa. *Tectonics* **10**, 1239–1256.

Ebinger, C., Poudjom-Djomani, Y., Mbede, E. & Foster, A. 1997 1991 Rifting the Archaean: development of the Natron–Manyara–Eyasi Basins, Tanzania. *J. Geol. Soc. Lond.* **154**, 947–960.

Forsyth, D. 1992 Finite extension and low angle normal faulting. *Geology* **20**, 27–30.

Foster, A. 1997 Seismicity and tectonics of Africa. PhD thesis, University of Cambridge, UK.

Foster, A. & Jackson, J. 1998 Source parameters of large African earthquakes: implications for crustal rheology and regional kinematics. *Geophys. J. Int.* **134**, 422–448.

Foster, A., Ebinger, C., Mbede, E. & Rex, D. 1997 Tectonic development of the northern Tanzanian sector of the East African Rift system. *J. Geol. Soc. Lond.* **154**, 689–700.

Gupta, A. & Scholz, C. H. 1998 Utility of elastic models in predicting fault displacement fields. *J. Geophys. Res.* **103**, 823–834

Hayward, N. 1996 A quantitative comparison of oceanic and continental rift segmentation. PhD thesis, University of Leeds, UK.

Hayward, N. & Ebinger, C. 1996 Variations in the along-axis segmentation of the Afar Rift system. *Tectonics* **15**, 244–257.

Hendrie, D., Kusznir, N., Morley, C. & Ebinger, C. 1994 A quantitative model of rift basin development in the northern Kenya Rift: evidence for the Turkana region as an 'accommodation zone' during the Palaeogene. *Tectonophys.* **236**, 409–438.

Jackson, J. & Blenkinsop, T. 1993 The Malawi earthquake of 10 March, 1989: deep faulting within the East African Rift system. *Tectonics* **12**, 1131–1139.

Jackson, J. & Blenkinsop, T. 1997 The Bilila–Mtakataka fault in Malawi: an active, 100 km long normal fault segment in thick seismogenic crust. *Tectonics* **16**, 137–150.

Jackson, J. & White, N. 1989 Normal faulting in the upper continental crust: observations from areas of active extension. *J. Struct. Geol.* **11**, 15–36.

Jestin, F., Huchon, P. & Gaulier, J. M. 1994 The Somali plate and the East African Rift system: present-day kinematics. *Geophys. J. Int.* **116**, 637–654.

Kikuchi, M. & Kanamori, H. 1995 The Shikotan earthquake of October 4, 1994: lithospheric earthquake. *Geophys. Res. Lett.* **22**, 1025–1028.

King, T. 1998 Tectonics and isostasy in extensional provinces: the Aegean Rifts. PhD thesis, University of Leeds, UK.

Kostrov, B. V. & Das, S. 1988 *Principles of earthquake source mechanics*. Cambridge University Press.

Last, R., Nyblade, A., Langston, C. & Owen, T. 1997 Crustal structure of the East African plateau from receiver functions and Rayleigh wave phase velocities. *J. Geophys. Res.* **102**, 24 469–24 483.

LeTurdu, C., Legall, B., Tiercelin, J.-J., Sturchio, N., Gente, P., Richert, J.-P. & Stead, D. 1999 A morphotectonic case study if a synrift extensional fault zone: the Baringo trachyte fault system, Central Kenya Rift. *Tectonophys.* (In the press.)

Ma, X. Q. & Kusznir, N. 1994 Effects of rigidity layering, gravity, and stress relaxation on 3D subsurface fault displacement fields. *Geophys. J. Int.* **118**, 210–220.

McKenzie, D. & Fairhead, F. 1997 Estimates of the effective elastic thickness of the continental lithosphere from Bouguer and free air gravity anomalies. *J. Geophys. Res.* **102**, 27 523–27 552.

Manighetti, I., Tapponnier, P., Gillot, P., Jacques, E., Courtillot, V., Armijo, R., Ruegg, J.-C. & King, G. C. P. 1998 Propagation of rifting along the Arabia–Somalia plate boundary: into Afar. *J. Geophys. Res.* **103**, 4947–4974.

Marty, B., Pik, R. & Gezahagen, Y. 1996 He isotopic variations in Ethiopian plume lavas: nature of magmatic sources and limit on lower mantle convection. *Earth Planet. Sci. Lett.* **144**, 223–237.

Mechie, J., Keller, G. R., Prodehl, C., Gaciri, S., Braile, L. W., Mooney, W. D., Gajewski, D. & Sandmeier, K.-J. 1994 Crustal structure beneath the Kenya Rift from axial profile data. In *Crustal and upper mantle structure of the Kenya Rift* (ed. C. Prodehl, G. R. Keller & M. A. Khan). *Tectonophys.* **236**, 179–200.

Menzies, M., Gallagher, K., Yelland, A. & Hurford, A. 1997 Volcanic and non-volcanic rifted margins of the Red Sea and Gulf of Aden: crustal cooling and margin evolution in Yemen. *Geochim. Cosmochim. Acta* **61**, 2511–2527.

Mohr, P. 1983 Ethiopian flood basalt province. *Nature* **303**, 577–584

Morley, C. K., Wescott, W. A., Stone, D., Harper, R. M., Wigger, S. T. & Karanja, F. 1992 Tectonic evolution of the northern Kenya Rift. *J. Geol. Soc. Lond.* **149**, 333–348.

Nyblade, A. & Langston, C. 1995 East African earthquakes below 20 km depth, and their implications for crustal structure. *Geophys. J. Int.* **121**, 49–62.

Nyblade, A., Pollack, H., Jones, D., Podmore, F. & Mushayandebvu, M. 1990 Terrestrial heat flow in East and southern Africa. *J. Geophys. Res.* **95**, 17 371–17 384.

Nyblade, A. A., Birt, C., Langston, C., Owens, T. & Last, R. 1996 Seismic experiment reveals rifting of craton in Tanzania. *Eos* **77**, 517–521.

Omar, G. I. & Steckler, M. S. 1995 Fission track evidence on the initial rifting of the Red Sea: two pulses, no propagation. *Science* **270**, 1341–1344.

Ori, G. G. 1989 Geologic history of the extensional basin of the Gulf of Corinth. *Geology* **17**, 918–921.

Petit, C. 1996 Le Rift Baikal et la collision Inde-Asie. PhD thesis, Geosciences Azur, University of Pierre et Marie Curie, Paris, France.

Ring, U. 1994 The influence of preexisting structure on the evolution of the Cenozoic Malawi Rift (East African Rift system). *Tectonics* **13**, 313–326.

Ritsema, J., Nyblade, A., Owens, T., Langston, C. & VanDecar, J. 1998 Upper mantle seismic velocity structure beneath Tanzania: implications for the stability of cratonic roots. *J. Geophys. Res.* **103**, 21 201–21 214.

Roberts, S. & Jackson, J. 1991 Active normal faulting in central Greece: an overview. In *The geometry of normal faults* (ed. A. Roberts, G. Yielding & B. Freeman). *Geol. Soc. Lond.* (Spec. Publ.) **56**, 125–142.

Rosendahl, B. R. 1987 Architecture of continental rifts with special reference to East Africa. *A. Rev. Earth Planet. Sci.* **15**, 445–503.

Ruegg, J.-C. (and 13 others) 1993 First epoch geodetic GPS measurements across the Afar plate boundary zone. *Geophys. Res. Lett.* **20**, 1899–1902.

Ruppel, C. 1995 Extensional processes in continental lithosphere. *J. Geophys. Res.* **100**, 24 187–24 215.

Ruppel, C., Kogan, M. & McNutt, M. 1993 Implications of new gravity data for Baikal Rift Structure. *Geophys. Res. Lett.* **20**, 1635–1638.

Schlische, R., Young, S., Ackermann, R. & Gupta, A. 1996 Geometry and scaling relations of a population of very small rift-related normal faults. *Geology* **24**, 683–686.

Scholz, C. H. 1988 The brittle-plastic transition and the depth of seismic faulting. *Geol. Rundsch.* **77**, 319–328.

Scholz, C. & Contreras, J. 1998 Mechanics of continental rift architecture. *Geology* **26**, 967–970.

Shackleton, R. 1993 Tectonics of the lower crust: a view from the Usambara mountains, NE Tanzania. *J. Struc. Geol.* **15**, 663–671.

Sigmundsson, F. 1992 Tectonic implications of the 1989 Afar earthquake sequence. *Geophys. Res. Lett.* **9**, 877–888.

Stein, R. & Barrientos, S. 1985 Planar high-angle normal faulting in the Basin and Range: geodetic analysis of the 1983 Borah Peak, Idaho, earthquake. *J. Geophys. Res.* **90**, 11 355–11 366.

Stewart, K. & Rogers, N. 1996 Mantle plume and lithosphere contributions to basalts from southern Ethiopia. *Earth Planet. Sci. Lett.* **139**, 195–211.

Theunissen, K., Klerkx, J., Melnikov, A. & Mruma, A. 1996, Mechanisms of inheritance of rift faulting in the western branch of the East African Rift, Tanzania. *Tectonics* **15**, 776–790.

Trudgill, B. & Cartwright, J. 1994. Relay-ramp forms and normal-fault linkages, Canyonlands National Park, Utah. *Geol. Soc. Am. Bull.* **106**, 1143–1157.

Upcott, N., Mukasa, R. K., Ebinger, C. & Karner, G. 1996 Along-axis segmentation and isostasy in the Western Rift, East Africa. *J. Geophys. Res.* **101**, 3247–3268.

van der Beek, P. 1997 Flank uplift and topography at the central Baikal Rift (SE Siberia): a test of kinematic models for continental extension. *Tectonics* **16**, 122–136.

van der Beek, P., Mbede, E., Andriessen, P. & Delvaux, D. 1998 Denudation history of the Malawi and Rukwa Rift flanks from apatite fission track thermochronology. *J. African Earth Sci.* **26**, 363–386.

Weissel, J. K. & Karner, G. 1989 Flexural uplift of rift flanks due to tectonic denudation of the lithosphere during extension. *J. Geophys Res.* **94**, 13 919–13 950.

Weissel, J., Malinverno, A., Harding, D. & Karner, G. 1995 Erosional development of the Ethiopian plateau of Northeast Africa from a fractal analysis of topography. In *Fractals in petroleum geology and earth processes* (ed. C. Barton & P. LaPointe), pp. 127–142. New York: Plenum.

Wheeler, W. & Karson, J. 1989 Structure and kinematics of the Livingstone Mountains Border Fault zone, Nyasa (Malawi) Rift, southwestern Tanzania. *J. African Earth Sci.* **8**, 393–413.

WoldeGabriel, G., Aronson, J. & Walter, R. C. 1990 Tectonic development of the Main Ethiopian Rift. *Geol. Soc. Am. Bull.* **102**, 439–458.

Yielding, G. 1985 Control of rupture by fault geometry during the El Asnam (Algeria) earthquake. *Geophys. J. R. Astr. Soc.* **81**, 641–670.

Zhao, M., Langston, C., Nyblade, A. & Owens, T. 1997 Lower crustal rifting in the Rukwa graben, East Africa. *Geophys. J. Int.* **129**, 412–420.

Discussion

D. McKenzie (*Bullard Laboratories, University of Cambridge, UK*). I'm intrigued by the relationship between the faulting and the volcanism. Once the spreading really gets going, it is perfectly reasonable that the scale of the segmentation is controlled by the total thickness of the melting zone. But at the beginning, for instance in East Africa, very small amounts of extension produce enormous volcanoes and long segments. How does that fit together? How do you get these enormous volcanoes when the amount of extension is so small?

C. J. Ebinger. There are large shield volcanoes along the length of the Eastern (Gregory) Rift, and a few large shields located within two isolated volcanic provinces of the Western Rift. One needs to have an extension, or beta, factor of about 1.5 to generate basalts by adiabatic decompression melting, whereas $\beta < 1.2$ in the Western Rift. Both the chemistry and volume of eruptive products and the gravity evidence for dynamic support of the East African and Ethiopian plateaux indicate that a mantle plume underlies East Africa, despite the lack of evidence for lithospheric thinning. The very small amount of extension with volcanism in the Western Rift need not be a problem, if we consider lateral flow of plume material along relief at the lithosphere–asthenosphere boundary, followed by decompression melting some distance from the plume source.

D. McKenzie. Well, that's not quite what's worrying me. In the southern part, where the amount of extension is very small, there is still a relationship between the individual volcanoes and the rift. Because the amount of extension is so small, it can scarcely have much influence on melt generation. Which means that, if there is a relationship, it has got to be the other way around, and the volcanoes control the rifting. This is to me a strange notion.

C. J. Ebinger. In the Rungwe region, the southernmost volcanic province in the Western Rift where $\beta \sim 1.1$, we can see that initial faulting was concurrent with, or occurred immediately after, initial volcanism. If volcanism is driving faulting, the *ca.* 600 km zone of extension without volcanism in the Western Rift is surely problematic. I would prefer to speculate that plume material rises and causes decompression melting above previously thinned lithosphere (e.g. Karoo Rifts), or steep gradients (e.g. craton boundaries), at the lithosphere–asthenosphere boundary. In this scenario, I would agree with you that magmatism locally is driving extension and contributes to the along-axis segmentation of the rift system, but it is not a prerequisite for generation of large normal fault systems.

N. Kusznir (*University of Liverpool, UK*). Is there a possibility that the small amount of rifting, while not enough to generate decompression melting, can actually control the plumbing? At the end of the developing rift segments there may be some tensile stresses that only affect the upper crust. However, these stresses may be enough to develop dilatancy in a tensile environment which just makes it easier for melts to get up there.

D. McKenzie. That is hard to do because the composition of the volcanoes I've looked at indicates that the melt is coming from the lithosphere and not from deeper down. I can see that if you were to produce melt from somewhere below the lithosphere, and then have some sort of channelling all the way up to the surface caused

by extension, you could divert it away from the craton but, from the volcanoes I have studied, it doesn't look as if the melt is coming from that deep.

K. E. Louden (*Dalhousie University, Halifax, Nova Scotia, Canada*). I have a simple question to ask. Some years ago I worked with gravity response functions to investigate various regions of oceanic crust. Through the work of Tony Watts and others, I felt that some understanding had been reached of the meaning of the effective thickness T_e for oceanic lithosphere. But I never really did have a very clear understanding of what T_e means for continental lithosphere. Is it the same? What does a T_e of 5 km mean for an old lithospheric centre like Africa?

C. J. Ebinger. In continental, as in oceanic regions, we represent the rheological properties of the compositionally layered lithosphere by an equivalent elastic thickness, the effective elastic thickness T_e, as a means to compare response functions from region to region. What the resulting effective elastic thickness then tells us about the rheology of the continental lithosphere is very difficult to assess, but we can say that variations in continental T_e values are dependent upon geothermal gradient, crustal composition, and strain rate.

A. B. Watts (*University of Oxford, UK*). Basically, what you are saying is that the range of elastic thickness values that you obtain reflects inheritance, in the sense that you've got higher values reflecting colder lithosphere and lower values reflecting warmer lithosphere. My point is that by the time we get to the case of oceanic crust formed by sea-floor spreading, or if you look at fault lengths over passive margins where you can actually measure the fault lengths, the fault lengths are already quite short, similar to the fault lengths that correspond to the low elastic thickness case. Also, the fault lengths on mid-ocean ridges themselves are very short. So, my question is, what is your view about what seems to happen when we go the extra step of forming an ocean? What is your view about what may happen to give us these very low values of elastic thickness in the passive margins?

C. J. Ebinger. Why are passive margins perpetually weak?

A. B. Watts. Yes, and in the Biscay section they have short fault lengths and look, elastically, like mid-ocean ridges.

C. J. Ebinger. To me, there are several possible interpretations of the patterns you describe. First, we see in the East African Rift system that a new along-axis segmentation can develop after considerable extension and magmatism has modified and heated the continental lithosphere. That is, originally long rift segments are preserved along the outer margin of the extensional province and a short segmentation, similar to mid-ocean ridge segmentation, is observed. One explanation, therefore, for the short fault lengths is the Afar analogy - a new short segmentation develops near the onset of sea-floor spreading, and is then perhaps a precursor of sea-floor spreading segmentation.

Second, one needs to look landward of passive margins to assess the role of strength during the initial stages of sea-floor spreading. Much of this record has been removed by as yet poorly understood erosion processes, making it difficult to assess the original border fault segment length during the initial stages of rifting. Studies of very young passive margins that developed in thermally stable lithosphere (e.g. Red Sea margins) may allow us to assess the temporal variability of border fault length implied by our Afar Rift studies.

Third, some passive margins may have been weak, hot rifts from the outset, with short fault segments, narrow syn-rift basins, and narrow rift flanks. In that case segments will appear similar to segmentation styles along mid-ocean ridges where the lithosphere was hot and weak at the time of fault initiation. Obviously, we need combined land and marine studies of conjugate margins to be able to answer these questions.

M. Menzies (*Royal Holloway College, University of London, UK*). What mechanism controls the orientation of the African Rift Valley and more importantly the Red Sea? Is there evidence for reactivation of basement (crustal) lineaments or is it a control from mantle structures (i.e. topography on the lithosphere–asthenosphere boundary)? The evidence from Yemen indicates that basement lineaments are at odds with the orientation of the Red Sea and very little evidence exists for reactivation of basement lineaments.

C. J. Ebinger. There are many papers comparing the trends of Precambrian lineaments detected in air photos and satellite imagery and the strikes of Late Cenozoic normal faults in East Africa that conclude a strong control of basement structures on rift faults. The few detailed studies of normal fault zones and basement structures provide a different story. Much of the Red Sea and East African Rift system has developed within accreted terrains and fold belts of the Pan-African system, and Cenozoic Rift faults often cut across Permo-Triassic and Cretaceous faults. Closer examination shows that steep Late Cenozoic Border Faults cross-cut Precambrian shear zones or metamorphic foliations showing shallower or highly variable dips, and that they cross-cut earlier border faults. Some segments of border faults may reactivate steep shear zones (e.g. Karonga Basin), or make jogs to follow pre-existing fractures, but the similarity of border fault and basin dimensions within sectors of the East African Rift, and other rifts worldwide, argues against a basement control. I would argue that favourably orientated pre-existing fractures and shear zones facilitate the propagation of border faults, rather than control their location and orientation.

A. Roberts (*Badleys Earth Sciences Ltd, Lincs, UK*). If the high values of T_e reported in this study are correct, you should be observing a radius of footwall uplift around individual faults of at least 100 km and possibly a lot more. I believe the rule of thumb is that the radius of footwall uplift will be about 10 times the effective elastic thickness. On seismic sections of buried basins, the radius of footwall uplift at basin margins is typically a few tens of kilometres, indicating low values of T_e in these situations. What is the radius of fault-controlled footwall uplift that you observe at the basin margins in this study?

C. J. Ebinger. The breadth of the uplifted rift flank, or radius of footwall uplift, is dependent on the effective elastic thickness, as well as interactions between footwall and hangingwall, beta-factor, and density of infilling material. Our forward models of basin and flank morphology for a T_e of 35 km predict an uplift radius of *ca.* 170 km, whereas those for a T_e of 10 km produce an uplift radius of *ca.* 60 km. These models provide good fits to the observed basin and flank morphology and to the gravity anomalies in the Western Rift, except in the immediate vicinity of the escarpment where erosional processes significantly modify the fault response (see figure 3). Referring back to your first statements, I would be surprised if seismic data of buried basins from the North Sea showed broad flanks, since these rifts did not develop in cratonic lithosphere.